Available online www.worldscientificnews.com

World Scientific News

An International Scientific Journal

WSN 208 (2025) 53-72 EISSN 2392-2192

Homotopy Analysis Method to Performance Study of Convective-Radiative Porous Fin with Internal Heat Generation under the Influence of Lorentz force

Gbeminiyi Sobamowo[1], Lawrence Jayesimi[2], Olanrewaju Isiaq[3], Carlos Agbelusi[4]

[1,4]Department of Mechanical Engineering, University of Lagos, Nigeria
[2] Works and Physical Planning Department, University of Lagos, Nigeria
[3]Department of Mechanical Engineering, Yaba College of Technology, Yaba, Lagos, Nigeria

ABSTRACT

In this work, the effect of magnetic field on nonlinear thermal performance of convective-radiative fin with temperature-dependent internal heat generation is analyzed using homotopy analysis method. The results of the series solutions are verified analytically and numerically, and very good agreements are established. The symbolic solutions are adopted to explore the impacts of the model parameters on the performance of the passive device. It is found that as the coductive-convective, conductive-radiative and magnetic field parameters increase, the fin temperature distribution in the fin decreases which the heat transfer rate through the fin is augmented and hence, the fin thermal efficiency is improved. The temperature distribution in the fin increases through the fin as the nonlinear thermal conductivity parameter increases. It is hoped that the present study gives a good insight into nonlinear analysis of the extended surface which will aid proper design of the extended surfaces in thermal systems.

Keywords: Analytical solution, Rectangular Fin, Temperature-dependent thermal conductivity, Homotopy Analysis Method.

(Received 23 August 2025; Accepted 15 September 2025; Date of Publication 6 October 2025)

1. INTRODUCTION

The non-expensive but effective cooling of electronics and thermal systems have been achieved through the applications of passive devices such as fins [1]. The importance of the extended surfaces has provoked a large volume of research in literatures. The theoretical investigations of thermal damage problems and heat transfer enhancement by the extended surfaces have attest to the facts that the controlling thermal models of the passive devices are always nonlinear. Consequently, the nonlinear thermal models have been successfully analyzed in the past studies with the aids of approximate analytical, semi-analytical, semi-numerical, and numerical methods. In such previous studies, Jordan et al. [8] adopted optimal linearization method to solve the nonlinear problems in the fin, while Kundu and Das [9] utilized Frobenius expanding series method for the analysis of the nonlinear thermal model of the fin. Khani et al. [10] and Amirkolaei and Ganji [11] applied homotopy analysis method. In a further analysis, Aziz and Bouaziz [12], Sobamowo [13], Ganji et al. [14] and Sobamowo et al. [15] employed methods of weighted residual to explore the nonlinear thermal behaviour of fins. In another studies, methods of double decomposition and variation of parameter were used by Sobamowo [16] and Sobamowo et al. [17], respectively, to study the thermal characteristics of fins. Also, differential transformation method has been used by some researchers such as Moradi and Ahmadikia [18], Sadri et al. [19], Ndlovu and Moitsheki [20], Mosayebidarchech et al. [21], Ghasemi et al. [22] and Ganji and Dogonchi [23] to predict the heat transfer behaviour in the passive devices. With the help of homotopy perturbation method, Sobamowo et al. [24], Arslanturk [25], Ganji et al. [26] and Hoshyar et al. [27] scrutinized the heat flow in the extended surfaces. However, these studies are for thermal analysis of fin under assumed constant heat transfer coefficient. The cases of heat transfer with variable heat transfer coefficient along the passive device varies has also be investigated [28-35]. Such analysis helps in providing the needed information on the efficiency, effectiveness, and design date of the extended surfaces under various boiling modes [33-44].

Since the thermal conductivities of fin materials are temperature-dependent, the influence of the temperature-dependent thermal properties on the performance of fin have been explored in past studies. However, Sobamowo et al. [45] presented in their work and showed some figures that show that the thermal conductivity of palladium is constant at a relatively low temperature. This depicts that the thermal performance of some materials has temperature-invariant thermal conductivity within some ranges of temperature. Moreover, influence of Lorentz force and temperature-variant internal heat generation on the temperature distribution of the extended surfaces is yet to be analyzed using homotopy analysis method. The analytical approach of homotopy analysis method reduces the complex mathematical analysis, high computational cost and time. Furthermore, under large values of thermo-geometric and nonlinear thermal conductivity parameters, it is established that applications of Adomian decomposition and homotopy perturbation methods are limited [46]. However, through an inherent property of auxiliary parameters for the adjustment and control of region and rate of convergence of approximate series solutions, homotopy analysis method has proven to be very an efficient and capable technique in handling nonlinear engineering problems in wider ranges of parameters. Therefore, the present work applies homotopy analysis method to provide analytical solution to the nonlinear heat transfer equation of convective-radiative fin with temperature-dependent thermal conductivity under the influences of magnetic field and with temperature-dependent internal heat generation. The developed symbolic solutions are used to examine the effects of the thermal model parameters on the performance of the fin.

2. PROBLEM FORMULATION

Consider a longitudinal rectangular fin with pores having convective and radiative heat transfer, as shown in Fig. 1. In order to derive the thermal model of the porous fin, it is assumed that the porous medium is isotropic, homogeneous, and it is saturated with single-phase fluid. The physical and thermal properties of the fin and the surrounding fluid surface are constant. The temperature varies in the fin is only along the length of the fin, as shown in Fig. 1. and there is a perfect contact between the fin base and the prime surface.

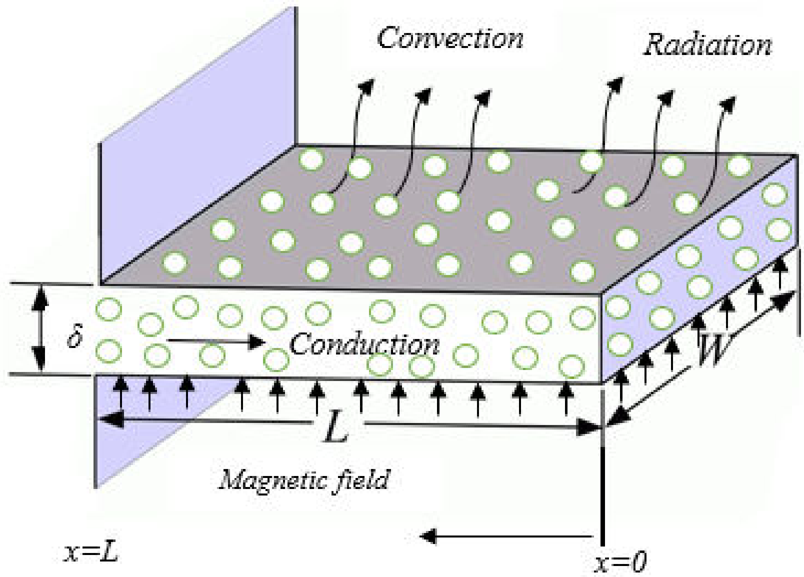

Figure 1. Schematic of convective-radiative longitudinal fin under even magnetic field.

From the assumptions and with the aid of Darcy's model, the energy balance is

$$\frac{d}{d\tilde{x}}\left(\frac{d\tilde{T}}{d\tilde{x}}+\frac{4\sigma}{3k_{eff}\beta_R}\frac{d\tilde{T}^4}{d\tilde{x}}\right)-\frac{\rho\beta c_p gK}{\nu k_{eff}A_{cr}}(\tilde{T}-T_a)^2-\frac{h(1-\varepsilon)P}{k_{eff}A_{cr}}(\tilde{T}-T_a)$$
$$-\frac{\sigma P\in}{k_{eff}A_{cr}}(\tilde{T}^4-T_a^4)-\frac{\mathbf{J_c}\times\mathbf{J_c}}{\sigma k_{eff}A_{cr}}A_s+\frac{q\left(\tilde{T}\right)}{k_{eff}}=0 \tag{1}$$

Expansion of the first term in Eq. (1), it provides

$$\frac{d^2\tilde{T}}{d\tilde{x}^2}+\frac{4\sigma}{3k_{eff}\beta_R}\frac{d}{d\tilde{x}}\left(\frac{d\tilde{T}^4}{d\tilde{x}}\right)-\frac{\rho\beta c_p gK}{\nu k_{eff}A_{cr}}(\tilde{T}-T_a)^2-\frac{h(1-\varepsilon)P}{k_{eff}A_{cr}}(\tilde{T}-T_a)$$
$$-\frac{\sigma P\in}{k_{eff}A_{cr}}(\tilde{T}^4-T_a^4)-\frac{\mathbf{J_c}\times\mathbf{J_c}}{\sigma k_{eff}A_{cr}}A_s+\frac{q\left(\tilde{T}\right)}{k_{eff}}=0 \tag{2}$$

The boundary conditions are

$$\tilde{x}=0,\quad \frac{d\tilde{T}}{d\tilde{x}}=0, \tag{3a}$$

$$\tilde{x}=L,\quad \tilde{T}=T_b \tag{3b}$$

The internal heat general varies linearly with temperature as

$$q(\tilde{T})=q_a\left(1+\lambda\left(\tilde{T}-T_a\right)\right) \tag{4}$$

When Eq. (4) is substituted into Eq. (2), one arrives at

$$\frac{d^2\tilde{T}}{d\tilde{x}^2}+\frac{4\sigma}{3k_{eff}\beta_R}\frac{d}{d\tilde{x}}\left(\frac{d\tilde{T}^4}{d\tilde{x}}\right)-\frac{\rho\beta c_p gK}{\nu\delta k_{eff}}(\tilde{T}-T_a)^2-\frac{h(1-\varepsilon)}{k_{eff}\delta}(\tilde{T}-T_a)$$
$$-\frac{\sigma\in}{k_{eff}\delta}(\tilde{T}^4-T_a^4)-\frac{\mathbf{J_c}\times\mathbf{J_c}}{\sigma k_{eff}A_{cr}}A_s+\frac{q_o}{k_{eff}}\left(1+\lambda\left(\tilde{T}-T_a\right)\right)=0 \tag{5}$$

The term T^4 can be expressed as a linear function of temperature as

$$\tilde{T}^4=T_a^4+4T_a^3\left(\tilde{T}-T_a\right)+6T_a^2\left(\tilde{T}-T_\infty\right)^2+\ldots\cong 4T_a^3\tilde{T}-3T_a^4 \tag{6}$$

Substitution of Eq. (6) into Eq. (5), results in

$$\frac{d^2\tilde{T}}{d\tilde{x}^2}+\frac{16\sigma}{3k_{eff}\beta_R}\frac{d^2\tilde{T}}{d\tilde{x}^2}-\frac{\rho\beta c_p gK}{\nu\delta k_{eff}}(\tilde{T}-T_a)^2-\frac{h(1-\varepsilon)}{k_{eff}\delta}(\tilde{T}-T_a)$$
$$-\frac{4\sigma T_a^3\in}{k_{eff}\delta}(\tilde{T}-T_a)-\frac{\mathbf{J_c}\times\mathbf{J_c}}{\sigma k_{eff}A_{cr}}A_s+\frac{q_o}{k_{eff}}\left(1+\lambda\left(\tilde{T}-T_a\right)\right)=0 \tag{7}$$

It should be noted that

$$\frac{\mathbf{J_c} \times \mathbf{J_c}}{\sigma} = \sigma_m B_o^2 u^2 \tag{8}$$

Therefore

$$\begin{aligned}&\frac{d^2\tilde{T}}{d\tilde{x}^2} + \frac{16\sigma}{3k_{eff}\beta_R}\frac{d^2\tilde{T}}{d\tilde{x}^2} - \frac{\rho\beta c_p gK}{v\delta k_{eff}}(\tilde{T}-T_a)^2 - \frac{h(1-\varepsilon)}{k_{eff}\delta}(\tilde{T}-T_a)\\&-\frac{\sigma T_a^3 \in}{k_{eff}\delta}(\tilde{T}-T_a) - \frac{\sigma_m B_o^2 u^2}{A_{cr}k_{eff}}A_s + \frac{q_o}{k_{eff}}\left(1+\lambda\left(\tilde{T}-T_a\right)\right) = 0\end{aligned} \tag{9}$$

Applying the following adimensional parameters in Eq. (10) to Eq. (9),

$$\begin{aligned}&X = \frac{\tilde{x}}{L},\ \theta = \frac{\tilde{T}-T_a}{T_b - T_a} \quad S = \frac{\rho\beta c_p gK}{k_{eff}\delta v}L^2 \quad M^2 = \frac{h(1-\varepsilon)L^2}{k_{eff}t} \quad Rd = \frac{4\sigma_{st}T_\infty^3}{3\beta_R k_{eff}} \quad N = \frac{4\sigma_{st} \in L^2 T_\infty^3}{k_{eff}t}.\\&H = \frac{\sigma A_s B_o^2 u^2 L^2}{A_{cr}k_{eff}},\ G = \frac{q_o t}{h\left(T_L - T_\infty\right)} \quad \gamma = \lambda(T_b - T_a)\end{aligned} \tag{10}$$

One arrives at the adimensional form of the governing Eq. (9) as presented in Eq. (11),

$$\frac{d^2\theta}{dX^2} + 4Rd\frac{d^2\theta}{dX^2} - S\theta^2 - M^2\theta - N\theta - H + M^2G\left(1+\gamma\theta\right) = 0 \tag{11}$$

and the adimensional boundary conditions

$$X = 0,\quad \frac{d\theta}{dX} = 0 \tag{12a}$$

$$X = 1,\quad \theta = 1 \tag{12b}$$

Taking

$$Mc^2 = \frac{M^2}{1+4Rd}, Nr = \frac{N}{1+4Rd},\ S_h = \frac{S}{1+4Rd},\ Ha = \frac{H}{1+4Rd},\ Q = \frac{G}{1+4Rd}, \tag{13}$$

we arrived at the dimensionless forms of the governing as follows;

$$\frac{d^2\theta}{dX^2} - S_h\theta^2 - Mc^2\theta - Nr\theta - Ha + Mc^2Q + Mc^2Q\gamma\theta = 0 \tag{14}$$

and the dimensionless boundary conditions still remain the same.

However, if the thermal conductivity of the material varies with temperature, we have

$$\frac{d^2\theta}{dX^2}+\beta\theta\frac{d^2\theta}{dX^2}+\beta\frac{d\theta}{dX}-S_h\theta^2-Mc^2\theta-Nr\theta-Ha+Mc^2Q+Mc^2Q\gamma\theta=0 \quad (15)$$

3. APPLICATION OF HOMOTOPY ANALYSIS METHOD TO THE THERMAL PROBLEM

It can be seen that the above governing differential equation is highly nonlinear, and such nonlinearity imposes some difficulties in the development of exact analytical methods to generate closed form solution for the equation. Therefore, homotopy analysis method is used in this work. The homotopy analysis method (HAM) which is an analytical scheme for providing approximate solutions to the ordinary differential equations, is adopted in generating solutions to the ordinary nonlinear differential equations .Upon constructing the homotopy, the initial guess and auxiliary linear operator can be expressed as

$$\theta_0(X)=1 \quad (16)$$

$$L(\theta)=\theta'' \quad (17)$$

$$L\left(c_1X+c_2\right)=0 \quad (18)$$

Where $c_i\left(i=1,2,3,4\right)$ are constants. Let $P=\in\left[0,1\right]$ connotes the embedding parameter and $\hbar$ is the non-zero auxiliary parameter. Therefore, the homotopy is constructed as

3.1. Zeroth-Order Deformation Equations

$$\left(1-p\right)L\left[\theta\left(X;p\right)-\theta_0(X)\right]=p\hbar H(X)N\left[\theta(X;p)\right] \quad (19)$$

$$\theta'(0;p)=0;\ \ \theta\left(1;p\right)=1; \quad (20)$$

when $p=0$ and $p=1$ we have

$$\theta(X;0)=\theta_0(X)\ ;\ \theta(X;1)=\theta(X) \quad (21)$$

As p increases from *0 to 1*. *θ(X;p)* varies from $\theta_o(X)$ to *θ(X)*. By Taylor's theorem and utilizing Eq. (20), *θ(X;p)* can be expanded in the power series of p as follows:

$$\theta(X;p)=\theta_0(X)+\sum_{m-1}^{\infty}\theta_m(X)p^m, \qquad \theta_m(X)=\frac{1}{m!}\frac{\partial^m(\theta(X;p))}{\partial p^m}\bigg|_{p=0} \quad (22)$$

where $\hbar$ is chosen such that the series is convergent at $p=1$; therefore, by Eq. (22) it is easily shown that

$$\theta(X)=\theta_0(X)+\sum_{m-1}^{\infty}\theta_m(X) \tag{23}$$

3.2. M-Th Order Deformation Equations

$$L[\theta_m(\eta)-\chi_m\theta_{m-1}(\eta)]=\hbar H(X)R_m(X) \tag{24}$$

$$\theta'(0;p)=0;\ \ \theta\left(1;p\right)=0; \tag{25}$$

Where

$$R_m(X)=\frac{d^2\theta\left(X;p\right)}{dX^2}-S_h\sum_{i=0}^{n-1}\theta_{n-1-k}\theta_k-Mc^2\theta_{n-1}-Nr\theta_{n-1}-Ha+Mc^2Q+Mc^2Q\gamma\theta_{n-1} \tag{26}$$

Now the results for the convergence, differential equation, and the auxiliary function are determined according to the solution expression. so we assume

$$H(X)=1 \tag{27}$$

The analytic solution is developed using the MATLAB computational stencil. Hence, the first deformation is expressed below

$$\theta_1(X)=\frac{1}{2}\hbar\left(-S_h-Mc^2+Mc^2Q+Mc^2Q\gamma-Ha\right)X^2+\frac{1}{2}\hbar S_h+\frac{1}{2}\hbar Mc^2-\frac{1}{2}\hbar Mc^2Q-\frac{1}{2}\hbar Mc^2Q\gamma+\frac{1}{2}\hbar Ha \tag{28}$$

$$\begin{aligned}\theta_2(X)=&\frac{5}{120}\hbar^2\left(-S_h-Mc^2+Mc^2Q+Mc^2Q\gamma-Ha\right)\left(-2S_h-Mc^2+M^2Q\gamma\right)X^4\\&+\frac{1}{2}\begin{bmatrix}-\hbar S_h-\hbar Mc^2+\hbar Mc^2Q-\hbar Ha+\frac{3}{2}\hbar^2S_hMc^2Q\gamma-\hbar^2S_h-\hbar^2Mc^2-\hbar^2S_h^2-\frac{1}{2}\hbar^2Mc^4+\hbar^2Mc^2Q-\hbar^2Ha-\frac{3}{2}\hbar^2S_hMc^2+\frac{1}{2}\hbar^2Mc^4Q\\-\frac{1}{2}\hbar^2Mc^2Ha+\hbar^2S_hMc^2Q-\hbar^2S_hHa+\hbar^2Mc^4Q\gamma+\hbar Mc^2Q\gamma-\frac{1}{2}\hbar^2Mc^4Q^2\gamma+\frac{1}{2}\hbar^2HaMc^2Q\gamma-\frac{1}{2}\hbar^2Mc^4Q^2\gamma^2+\hbar^2Mc^2Q\gamma\end{bmatrix}X^2\\&+\frac{5}{24}\hbar^2Mc^4-\frac{1}{2}\hbar^2Mc^2Q+\frac{5}{8}\hbar^2Mc^2-\frac{5}{24}\hbar^2Mc^4Q+\frac{5}{24}\hbar^2Mc^2Ha+\frac{1}{2}\hbar Mc^2+\frac{5}{24}\hbar^2Mc^4Q^2\gamma^2-\frac{5}{12}\hbar^2S_hMc^2Q+\frac{5}{12}\hbar^2S_hHa-\frac{5}{12}\hbar^2Mc^4Q\gamma\\&+\frac{5}{12}\hbar^2Mc^4Q^2\gamma-\frac{1}{2}\hbar^2Mc^2Q\gamma-\frac{1}{2}\hbar Mc^2Q\gamma-\frac{1}{2}\hbar Mc^2Q+\frac{1}{2}\hbar^2Ha-\frac{5}{8}\hbar^2S_hMc^2Q\gamma+\frac{1}{2}\hbar^2S_h+\frac{1}{2}\hbar^2Mc^2+\frac{1}{2}\hbar S_h+\frac{5}{12}\hbar^2S_h^2\end{aligned} \tag{29}$$

Similarly $\theta_3(\eta)$, $\theta_4(\eta)$, $\theta_5(\eta)$... are found, but they are too large expressions that cannot be included in this paper. However, they are included in the results displayed graphically. From the principle of HAM

$$\theta(X)=\theta_0(X)+\sum_{m=1}^{\infty}\theta_m(X)=\theta_0(X)+\theta_1(X)+\theta_2(X)+\ldots \tag{30}$$

Therefore, substitute Eqs. (16), (28) and 29) into Eq. (30), we have

$$\theta(X)=1+\frac{1}{2}\hbar\left(-S_h-Mc^2+M^2Q+M^2Q\gamma-Ha\right)X^2+\frac{1}{2}\hbar S_h+\frac{1}{2}\hbar Mc^2-\frac{1}{2}\hbar Mc^2Q-\frac{1}{2}\hbar Mc^2Q\gamma+\frac{1}{2}\hbar Ha$$
$$+\frac{5}{120}\hbar^2\left(-S_h-Mc^2+M^2Q+Mc^2Q\gamma-Ha\right)\left(-2S_h-Mc^2+Mc^2Q\gamma\right)X^4$$
$$+\frac{1}{2}\begin{bmatrix}-\hbar S_h-\hbar Mc^2+\hbar Mc^2Q-\hbar Ha+\frac{3}{2}\hbar^2S_hMc^2Q\gamma-\hbar^2S_h-\hbar^2Mc^2-\hbar^2S_h^2-\frac{1}{2}\hbar^2Mc^4+\hbar^2Mc^2Q-\hbar^2Ha-\frac{3}{2}\hbar^2S_hMc^2+\frac{1}{2}\hbar^2Mc^4Q\\-\frac{1}{2}\hbar^2Mc^2Ha+\hbar^2S_hMc^2Q-\hbar^2S_hHa+\hbar^2Mc^4Q\gamma+\hbar Mc^2Q\gamma-\frac{1}{2}\hbar^2Mc^4Q^2\gamma+\frac{1}{2}\hbar^2HaMc^2Q\gamma-\frac{1}{2}\hbar^2Mc^4Q^2\gamma^2+\hbar^2Mc^2Q\gamma\end{bmatrix}X^2$$
$$+\frac{5}{24}\hbar^2Mc^4-\frac{1}{2}\hbar^2Mc^2Q+\frac{5}{8}\hbar^2Mc^2-\frac{5}{24}\hbar^2Mc^4Q+\frac{5}{24}\hbar^2Mc^2Ha+\frac{1}{2}\hbar Mc^2+\frac{5}{24}\hbar^2Mc^4Q^2\gamma^2-\frac{5}{12}\hbar^2S_hMc^2Q+\frac{5}{12}\hbar^2S_hHa-\frac{5}{12}\hbar^2Mc^4Q\gamma$$
$$+\frac{5}{12}\hbar^2Mc^4Q^2\gamma-\frac{1}{2}\hbar^2Mc^2Q\gamma-\frac{1}{2}\hbar Mc^2Q\gamma-\frac{1}{2}\hbar Mc^2Q+\frac{1}{2}\hbar^2Ha-\frac{5}{8}\hbar^2S_hMc^2Q\gamma+\frac{1}{2}\hbar^2S_h+\frac{1}{2}\hbar^2Mc^2+\frac{1}{2}\hbar S_h+\frac{5}{12}\hbar^2S_h^2+\ldots$$

(31)

4. CONVERGENCE OF THE HAM SOLUTION

In order to control the convergence rate of $\hbar$ in the approximate analytical solutions given by HAM, Liao [47] presented the auxiliary parameter. It is established that the convergence rate of approximation for the HAM solution strongly depend on the value of the auxiliary parameter. For the 10th-order of approximation, different values of the model parameters are used for the different simulations to arrive at the acceptable range of values of the parameter $\hbar$ for the difference controlling parameters of the model.

5. NUMERICAL PROCEDURE FOR THE ANALYSIS OF THE GOVERNING EQUATION

In order to verify the results of the present work, the nonlinear model in Eq. (9) was also solved numerically using fifth-order Runge-Kutta Fehlberg method (Cash-Karp Runge-Kutta) coupled with shooting method. Since Runge-Kutta method is for solving first-order ordinary differential equation, the fourth-order ordinary differential equation is decomposed into a system of first-order differential equations as follows:

$$\theta'=p,\qquad \Rightarrow\theta''=p', \tag{32}$$

$$p'=S_h\theta^2+Mc^2\theta+Nr\theta+Ha-Mc^2Q-Mc^2Q\gamma\theta \tag{33}$$

The above Eqs. (30) and (31) can be written as

$$f\left(X,\theta,p\right)=p, \tag{34}$$

$$g\left(X,\theta,p\right)=S_h\theta^2+Mc^2\theta+Nr\theta+Ha-Mc^2Q-Mc^2Q\gamma\theta,$$

The iterative scheme of the fifth-order Runge-Kutta Fehlberg method (Cash-Karp Runge-Kutta) for the above system of first-order equations is given as

$$\theta_{i+1}=\theta_i+h\left(\frac{2835}{27648}k_1+\frac{18575}{48384}k_3+\frac{13525}{55296}k_4+\frac{277}{14336}k_5+\frac{1}{4}k_6\right) \tag{35}$$

$$p_{i+1} = p_i + h\left(\frac{2835}{27648}l_1 + \frac{18575}{48384}l_3 + \frac{13525}{55296}l_4 + \frac{277}{14336}l_5 + \frac{1}{4}l_6\right) \tag{36}$$

where

$$k_1 = f\left(X_i, \theta_i, p_i\right)$$

$$l_1 = g\left(X_i, \theta_i, p_i\right)$$

$$k_2 = f\left(X_i + \frac{1}{5}h,\ \theta_i + \frac{1}{5}k_1 h,\ p_i + \frac{1}{5}l_1 h\right)$$

$$l_2 = g\left(X_i + \frac{1}{5}h,\ \theta_i + \frac{1}{5}k_1 h,\ p_i + \frac{1}{5}l_1 h\right)$$

$$k_3 = f\left(X_i + \frac{3}{10}h,\ \theta_i + \frac{3}{40}k_1 h + \frac{9}{40}k_2 h,\ \ p_i + \frac{3}{40}l_1 h + \frac{9}{40}l_2 h\right)$$

$$l_3 = g\left(X_i + \frac{3}{10}h,\ \theta_i + \frac{3}{40}k_1 h + \frac{9}{40}k_2 h,\ \ p_i + \frac{3}{40}l_1 h + \frac{9}{40}l_2 h\right)$$

$$k_4 = f\left(X_i + \frac{3}{5}h,\ \theta_i + \frac{3}{10}k_1 h - \frac{9}{10}k_2 h + \frac{6}{5}k_3 h,\ \ p_i + \frac{3}{10}l_1 h - \frac{9}{10}l_2 h + \frac{6}{5}l_3 h\right)$$

$$l_4 = g\left(X_i + \frac{3}{5}h,\ \theta_i + \frac{3}{10}k_1 h - \frac{9}{10}k_2 h + \frac{6}{5}k_3 h,\ \ p_i + \frac{3}{10}l_1 h - \frac{9}{10}l_2 h + \frac{6}{5}l_3 h\right)$$

$$k_5 = f\left(X_i + h,\ \theta_i - \frac{11}{54}k_1 h + \frac{5}{2}k_2 h - \frac{70}{27}k_3 h + \frac{35}{27}k_4 h,\ \ p_i - \frac{11}{54}l_1 h + \frac{5}{2}l_2 h - \frac{70}{27}l_3 h + \frac{35}{27}l_4 h\right)$$

$$l_5 = g\left(X_i + h,\ \theta_i - \frac{11}{54}k_1 h + \frac{5}{2}k_2 h - \frac{70}{27}k_3 h + \frac{35}{27}k_4 h,\ \ p_i - \frac{11}{54}l_1 h + \frac{5}{2}l_2 h - \frac{70}{27}l_3 h + \frac{35}{27}l_4 h\right)$$

$$k_6 = f\begin{pmatrix} X_i + \frac{7}{8}h,\ \theta_i + \frac{1631}{55296}k_1 h + \frac{175}{512}k_2 h + \frac{575}{13824}k_3 h + \frac{44275}{110592}k_4 h + \frac{253}{4096}k_5 h, \\ p_i + \frac{1631}{55296}l_1 h + \frac{175}{512}l_2 h + \frac{575}{13824}l_3 h + \frac{44275}{110592}l_4 h + \frac{253}{4096}l_5 h, \end{pmatrix}$$

$$l_6 = g\begin{pmatrix} X_i + \frac{7}{8}h,\ \theta_i + \frac{1631}{55296}k_1 h + \frac{175}{512}k_2 h + \frac{575}{13824}k_3 h + \frac{44275}{110592}k_4 h + \frac{253}{4096}k_5 h, \\ p_i + \frac{1631}{55296}l_1 h + \frac{175}{512}l_2 h + \frac{575}{13824}l_3 h + \frac{44275}{110592}l_4 h + \frac{253}{4096}l_5 h, \end{pmatrix}$$

Using the above fifth-order Runge-Kutta Fehlberg method coupled with shooting method, computer programs are written in MATLAB for the solutions of the Eq. (9). The results for step size, $h = 0.01$ are presented in the following section.

6. PARAMETERS OF ENGINEERING INTERESTS

In this section, the parameters of engineering Interest for the thermal problem are presented.

6.1. Heat Flux and Efficiency Models of the Fin

The fin base heat flux is given by

$$q_{bn} = A_c k \frac{dT}{dx} \tag{37}$$

Using the dimensionless parameters in Eq. (10), at the base of the fin, the dimensionless heat transfer rate is developed as

$$q_b = \frac{q_{bn} L}{k_a A_c (T_b - T_\infty)} = \frac{d\theta}{dX} \tag{38}$$

The total heat flux of the fin is given by

$$q_T = \frac{q_b}{A_c h(T - T_b)} \tag{39}$$

After substitution of Eq. (39) and using the dimensionless parameters in Eq. (10), one arrives at

$$q_T = \frac{1}{Bi}\frac{k}{h}\frac{d\theta}{dX} = \frac{1}{Bi}\frac{d\theta}{dX} \tag{40}$$

The fin efficiency is the ratio of the rate of heat transfer rate by the fin to the rate of heat transfer that would be if the entire fin were at the base temperature and is given by

$$\eta = \frac{\int_0^1 \left[\frac{\rho c_p g K \beta_p sin(\gamma)(T - T_a)^2}{k_{eff} t v} + \frac{h(T - T_a)}{k_{eff} t} + \frac{4\sigma\varepsilon T_a^3 (T - T_a)}{k_{eff} t} + \frac{\sigma B_o^2 u^2 A_s}{k_{eff} A_{cr}} \right] dx}{\frac{\rho c_p g K \beta_p (T_b - T_a)^2}{k_{eff} t v} + \frac{h(T_b - T_a)}{k_{eff} t} + \frac{4\sigma\varepsilon T_a^3 (T_b - T_a)}{k_{eff} t} + \frac{\sigma B_o^2 u^2 A_s}{k_{eff} A_{cr}}} \tag{41}$$

Using the adimensional parameters in Eq. (10), we arrived at

$$\eta = \frac{S\int_0^1 \theta^2 dX + \left\{ M^2 + Nr \right\} \int_0^1 \theta dX + H\int_0^1 dX}{S + M^2 + Nr + Ha} \tag{42}$$

Which gives

$$\eta = \frac{S\int_0^1 \theta^2 dX + \left\{M^2 + Nr\right\}\int_0^1 \theta dX + Ha}{S + M^2 + Nr + Ha} \tag{43}$$

7. RESULTS AND DISCUSSION

The numerical solutions are coded in MATLAB, and the parametric and sensitivity analyses are carried out using the codes. The parametric results are presented in Fig. 2-11.

Fig. 2 reveals that the fin temperature decreases when the magnetic field parameter increases. This is because when the magnetic field parameter increases, there is an increase Lorentz force which provides resistive force that opposes motion of the working fluid around the fin and consequently, the fin temperature decreases.

It is illustrated in Fig. 3 and 4 about the influence of thermal conductivity parameters on the adimensional temperature profiles. The adimensional temperature distribution in the fin increases with increase in thermal conductivity parameter. It should be well pointed out that when $\beta = 0$ it implies a constant or temperature-invariant thermal conductivity. The figure depicts that under the scenario of constant thermal conductivity, the fin achieves a lowest temperature distribution. Also, at such thermal conductivity that is temperature-invariant, steepest temperature gradient is achieved in the temperature profile. Therefore, thermal conductivity of a material contributes significantly to the temperature difference between the fin base and its tip. This is because the thermal conductivity determines the thermal resistance that a material produces. Additionally, difference in temperature between the fin base and its tip is amplified when thermo-geometric parameters such as the conductive-convective, conductive-radiative and porous parameters increase. It should be announced under temperature-invariant thermal conductivity and maintaining constant fin properties and the external conditions, the fin thermal efficiency will remain constant when the fin temperature increases within the temperature range of constant thermal conductivity of the material.

The impact of porous parameter on the adimensional temperature is presented in Fig. 5 and 6. It is shown in the figures that when the porosity parameter increases, the adimensional fin temperature decreases and the heat transfer rate through the fin increases . Fig. 7, 8 and 9 show the influence of temperature-dependent thermal conductivity parameter on the adimensional heat transfer rate at the base of the fin at different radiation parameters. Fig. 10 shows that increase in the thermal conductivity parameter, the heat transfer rate through the fin and the thermal efficiency of the fin increase. Fin is more efficient and effective for larger value of thermal conductivity. This trend was also depicted in Fig. 11.

The present results from the simulations show that through an inherent property of auxiliary parameters for the adjustment and control of region and rate of convergence of approximate series solutions, homotopy analysis method has proven to be very an efficient and capable technique in handling nonlinear engineering problems in wider ranges of parameters. However, when the values of thermo-geometric and nonlinear thermal conductivity parameters are large, it is established that applications of Adomian decomposition and homotopy perturbation methods are limited [46].

Table 1. Comparison of results

X	HAM	NUM	| NM – HAM |
0.00	0.863499664	0.863499231	0.000000433
0.05	0.863829046	0.863828568	0.000000478
0.10	0.864817539	0.864817090	0.000000449
0.15	0.866466182	0.866465743	0.000000439
0.20	0.868776709	0.868776261	0.000000448
0.25	0.871751555	0.871751104	0.000000451
0.30	0.875393859	0.875393404	0.000000455
0.35	0.879707472	0.879707010	0.000000462
0.40	0.884696967	0.884696500	0.000000467
0.45	0.890367650	0.890367181	0.000000469
0.50	0.896725569	0.896725096	0.000000473
0.55	0.903777531	0.903777060	0.000000471
0.60	0.911531120	0.911530658	0.000000462
0.65	0.919994710	0.919994259	0.000000451
0.70	0.929177488	0.929177056	0.000000432
0.75	0.939089476	0.939089079	0.000000397
0.80	0.949741555	0.949741203	0.000000352
0.85	0.961145491	0.961145189	0.000000302
0.90	0.973313964	0.973313764	0.000000200
0.95	0.986260599	0.986260549	0.000000005
1.00	1.000000000	1.000000000	0.000000000

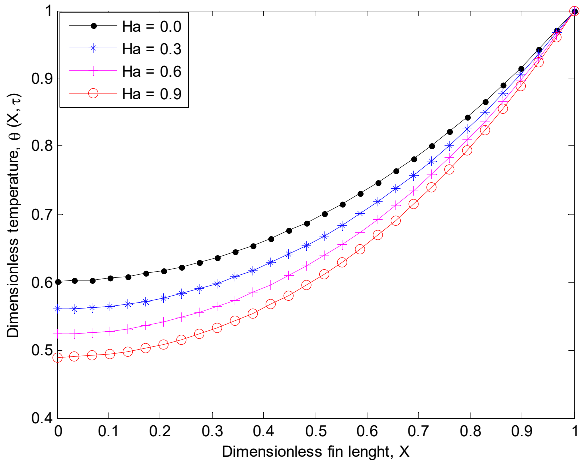

Figure 2. Impacts of magnetic field parameter on fin thermal distribution.

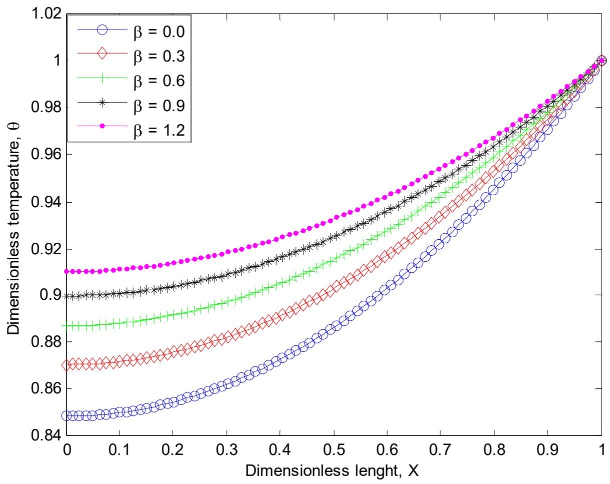

Figure 3. Dimensionless temperature distribution in the fin parameters for varying thermo-geometric parameter. when S_h,= 0.2, M=0.4

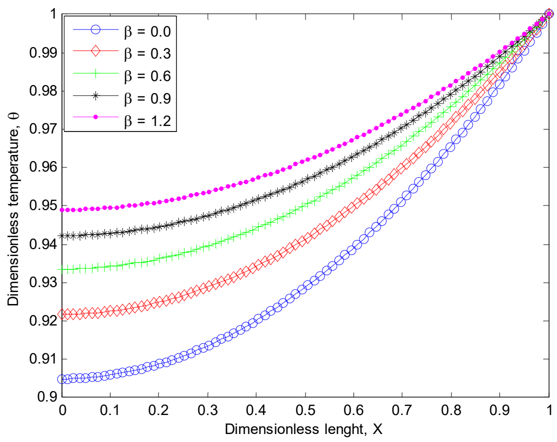

Figure 4. Dimensionless temperature distribution in the fin parameters for varying thermo-geometric parameter when S_h,= 0.1, M=0.4.

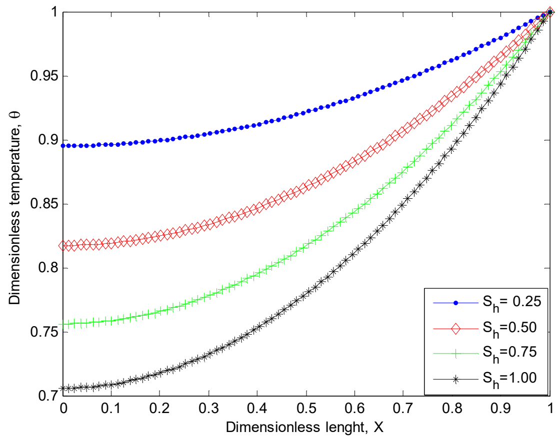

Figure 5. Dimensionless temperature distribution in the fin parameters for varying thermo-geometric parameter for constant thermal conductivity.

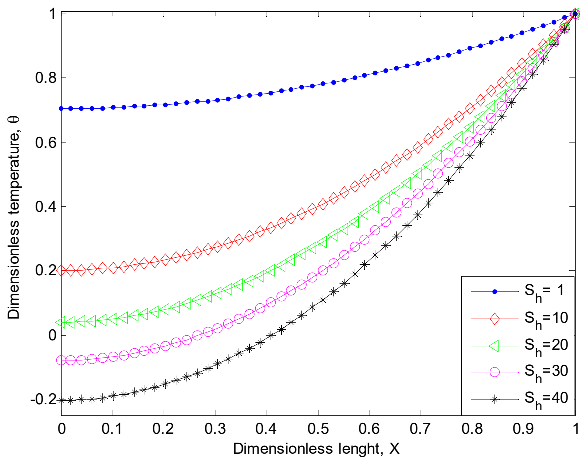

Figure 6. Effects of porous parameter on the temperature distribution in the fin parameters for constant thermal conductivity.

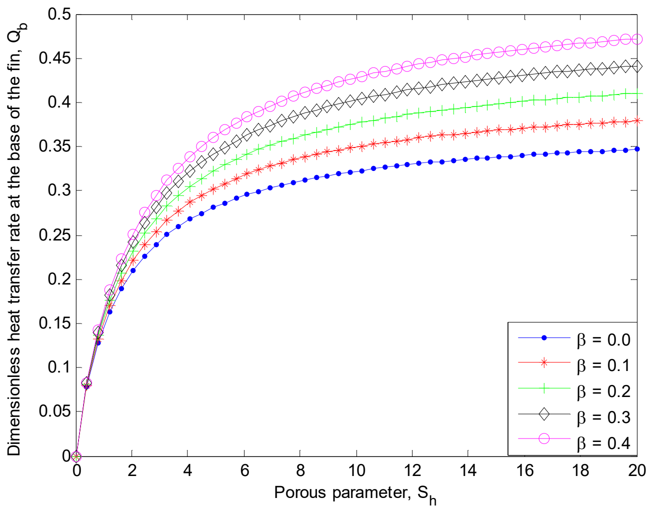

Figure 7. Effects of thermal conductivity and porosity on heat flux when Mc=0.5, Nr=0.2.

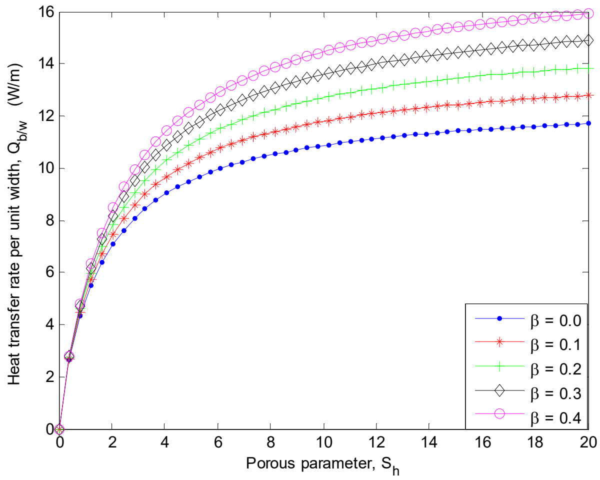

Figure 8. Effects of thermal conductivity and porosity on heat flux when Mc=2, Nr=0.3.

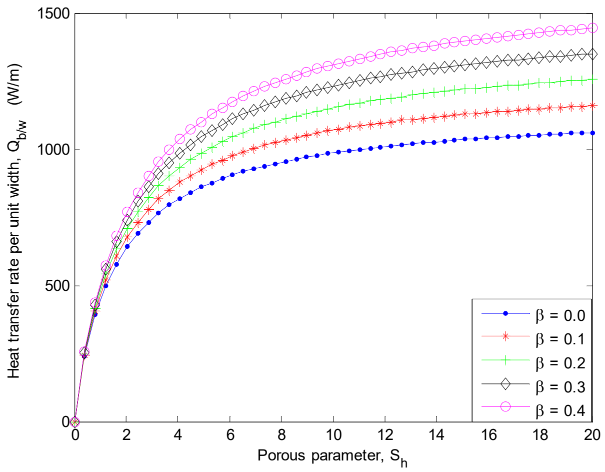

Figure 9. Effects of thermal conductivity and porosity on heat flux when Mc=2.5, Nr=0.4.

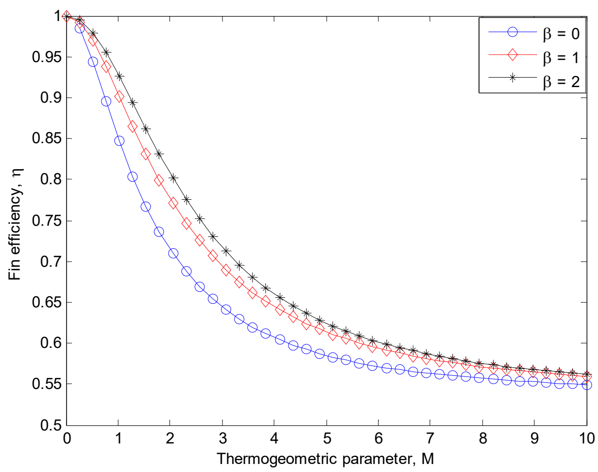

Figure 10. Effects of thermal conductivity and conductive-convective parameter on the fin efficiency when Mc=2, N=0.2, S=0.5.

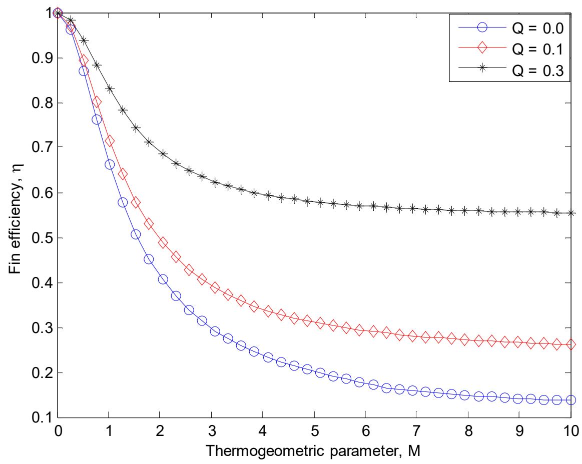

Figure 11. Effect of internal heat generation on the fin efficiency when Sh=0.5, Nr=0.2, γ=0.8.

8. CONCLUSION

In this work, thermal performance of convective-radiative internally heated porous fin subjected to magnetic field has been analyzed using homotopy analysis method. The results of the homotopy analysis method are in excellent agreement with the results of the fifth-order Runge-Kutta Fehlberg method (Cash-Karp Runge-Kutta) coupled with shooting method. From the study, it is found that increase in magnetic field, porosity, convective, radiative, and magnetic parameters fin cause the temperature to decrease and increase the rate of heat transfer from the fin and consequently improve the efficiency of the fin. The homotopy analysis method gives the freedom of choosing the best the auxiliary parameter that could be used to adjust and control the convergence of the series solution. Such freedom of choice is not offered in the other approximate analytics methods.

Nomenclature

A_{cr} fin cross sectional area, m^2
B_o magnetic field intensity,, Tesla or kg/sec^2Amp
c_{pa} specific heat capacity, J/kgK
h coefficient of convective heat transfer, W/m^2K
J_c conduction current intensity, A
k fin thermal conductivity, W/mK
k_b fin thermal conductivity at the base temperature, W/mK
L fin length, M
Mc adimensional convective parameter
Nr adimensional radiation parameter
P fin perimeter, m
t time, sec.
T fin temperature, K
T_∞ ambient temperature, K
T_b fin temperature at the base, K
x fin axial distance, m
X adimensional fin length

Greek Symbols

δ fin thickness, m
θ adimensional temperature
θ_b adimensional temperature at the fin base
ρ fin material density, kg/m^3
σ Stefan-Boltzmann constant, W/m^2K^4
σ Electrical conductivity, $\Omega^{-1}m^{-1}$ or sec^2Amp^2/kgm^3

References

[1] S. Kiwan, A. Al-Nimr. Using Porous Fins for Heat Transfer Enhancement. ASME J. Heat Transfer 2001; 123:790–5.

[2] S. Kiwan, Effect of radiative losses on the heat transfer from porous fins. Int. J. Therm. Sci. 46(2007a)., 1046-1055

[3] S. Kiwan, O. Zeitoun, Natural convection in a horizontal cylindrical annulus using porous fins. Int. J. Numer. Heat Fluid Flow 18 (5)(2008), 618-634.

[4] S. Kiwan. Thermal analysis of natural convection porous fins. Tran. Porous Media 67(2007b), 17-29.

[5] R. S. Gorla, A. Y. Bakier. Thermal analysis of natural convection and radiation in porous fins. Int. Commun. Heat Mass Transfer 38(2011), 638-645.

[6] B. Kundu, D. Bhanja, K. S. Lee. A model on the basis of analytics for computing maximum heat transfer in porous fins. Int. J. Heat Mass Transfer 55 (25-26)(2012) 7611-7622.

[7] M. T. Darvishi, R. Gorla, R.S., Khani, F., Aziz, A.-E. Thermal performance of a porus radial fin with natural convection and radiative heat losses. Thermal Science, 19(2) (2015) 669-678.

[8] A. Jordan, S. Khaldi, M. Benmouna, A. Borucki. Study of non-linear heat transfer problems, Revue Phys. Appl., 22(1987),101-105.

[9] B. Kundu, P.K. Das. Performance analysis and optimization of straight taper fins with variable heat transfer coefficient, International Journal of Heat and Mass Transfer, 45(2002), 4739- 4751.

[10] F. Khani, M. A. Raji, H. H. Nejad. Analytical solutions and efficiency of the nonlinear fin problem with temperature-dependent thermal conductivity and heat transfer coefficient, Commun Nonlinear Sci Numer Simulat, 14(2009), 3327-3338.

[11] S. R. Amirkolei and D. D. Ganji D.D. Thermal performance of a trapezoidal and rectangular profiles fin with temperature-dependent heat transfer coefficient, thermal conductivity and emissivity, Indian J. Sci. Res., 1(2)(2014), 223-229.

[12] A. Aziz, M. N. Bouaziz. A least squares method for a longitudinal fin with temperature dependent internal heat generation and thermal conductivity, Energy Conversion and Management, 52(2011), 2876-2882.

[13] M. G. Sobamowo. Thermal analysis of longitudinal fin with temperature dependent properties and internal heat generation using Galerkin's method of weighted residual, Applied Thermal Engineering, 99(2016), 1316-1330.

[14] D. D. Ganji, M. Raghoshay, M. Rahimi, M. Jafari. Numerical investigation of fin efficiency and temperature distribution of conductive, convective and radiative straight fins, IJRRAS, 2010, 230-237.

[15] M. G. Sobamowo, O. M. Kamiyo and O. A. Adeleye. Thermal performance analysis of a natural convection porous fin with temperature-dependent thermal conductivity and internal heat generation. Thermal Science and Engineering Progress. 1(2017) 39-52.

[16] M. G. Sobamowo. Thermal performance and optimum design analysis of fin with variable thermal conductivity using double decomposition method. Journal of Mechanical Engineering and Technology. 9(1)(2017), 1-32.

[17] M. G. Sobamowo, L. O. Jayesimi and J. D. Femi-Oyetoro. Heat transfer study in a convective-radiative fin with temperature-dependent thermal conductivity and magnetic field using variation of parameter method. Journal of Applied Mathematics and Computational Mechanics, 16(3)(2017), 85-96.

[18] A. Moradi and H. Ahmadikia. Analytical solution for different profiles of fin with temperature dependent thermal conductivity, Mathematical Problems in Engineering, 2010, 1-15

[19] S. Sadri, M. R. Raveshi and S. Amiri. Efficiency analysis of straight fin with variable heat transfer coefficient and thermal conductivity, Journal of Mechanical Science and Technology, 26(4)(2011), 1283-1290.

[20] P. L. Ndlovu and R. J. Moitsheki. Analytical solutions for steady heat transfer in longitudinal fins with temperature dependent properties, Mathematical Problems in Engineering, 2013, 1-14.

[21] S. Mosayebidorcheh, D. D. Ganji, M. Farzinpoor. Approximate solution of the nonlinear heat transfer equation of a fin with the power-law temperature- dependent thermal conductivity and heat transfer coefficient, Propulsion and Power Research, 3(1)(2014), 41-47.

[22] S. E. Ghasemi, M. Hatami, D. D. Ganji. Thermal analysis of convective fin with temperature-dependent thermal conductivity and heat generation, Case Studies in Thermal Engineering, 4(2014), 1-8.

[23] D.D. Ganji and A.S. Dogonchi. Analytical investigation of convective heat transfer of a longitudinal fin with temperature- dependent thermal conductivity, heat transfer coefficient and heat generation, International Journal of Physical Sciences, 9(21) (2014), 466-474.

[24] [24]. M. G. Sobamowo, O. A. Adeleye and A. A. Yinusa. Analysis of convective-radiative porous fin with temperature-dependent internal heat generation and magnetic using homotopy perturbation method. Journal of computational and Applied Mechanics. 12(2)(2017), 127-145.

[25] C. Arslanturk. Optimization of straight fins with step change in thickness and variable thermal conductivity by homotopy perturbation method, J. of Thermal Science and Technology, 10(2010), 9-19.

[26] D. D. Ganji, Z. Z. Ganji, H. D. Ganji (2011). Determination of temperature distribution for annular fins with temperature dependent thermal conductivity by HPM, Thermal Science, 15(1)(2011), 111-115.

[27] H. A. Hoshyar, I. Rahimipetroudi, D. D. Ganji, A. R. Majidian. Thermal performance of porous fins with temperature-dependent heat generation via the homotopy perturbation method and collocation method, Journal of Applied Mathematics and Computational Mechanics, 14(4)(2015), 53-65.

[28] K. W. Haley; J. W. Westwater. Boiling heat transfer from a single fin to a boiling liquid. Chem. Eng. Sci. 20(1965): 711

[29] F. S. Lai, Y. Y. Hsu. Temperature distribution in a fin partially cooled by nucleate boiling. AIChE J. 13(1967): 817-821

[30] A. D. Kraus AD (1988) Sixty-five years of extended surface technology. Appl. Mech. Rev. 41(1988): 321-364

[31] S. P. Liaw, R. H. Yeh. Fins with temperature dependent surface heat flux-I. Single heat transfer mode. Int. J. Heat Mass Transfer 37(1994), 1509-1514

[32] S. P. Liaw SP; R. H. Yeh. Fins with temperature dependent surface heat flux-II. Multi-boiling heat transfer, Int. J. Heat Mass Transfer 37(1994): 1517-1524

[33] H. C. Unal HC (1985) Determination of the temperature distribution in an extended surface with a non-uniform heat transfer coefficient. Int. J. Heat Mass Transfer 28(1985): 2279-2284

[34] H. C. Unal. Determination of the temperature distribution in an extended surface with a non-uniform heat transfer coefficient, Int. J. Heat Mass Transfer, 28(1986), 2279-2284.

[35] H. C. Unal. A simple method of dimensioning straight fins for nucleate pool boiling, Int. J. Heat Mass Transfer, 29(1987), 640-644, 1987.

[36] H. C. Unal. An analytic study of boiling heat transfer from a fin, Int. J. Heat Mass Transfer, 30(1987), 341-349.

[37] R. H. Yeh, S. P. Liaw. (1990) An exact solution for thermal characteristics of fins with power-law heat transfer coefficient. Int. Comm. Heat Mass Transfer 17(1990): 317 330

[38] A. K. Sen, S. Trinh. An exact solution for the rate of heat transfer from a rectangular fin governed by power law-type temperature dependence. ASME J. Heat Transfer 108(1986): 457-459

[39] S. P. Liaw, R. H. Yeh. Analysis of pool boiling heat transfer on a single cylindrical fin. J. Chin. Soc. Mech. Eng. 11(1990): 448-454

[40] R. H. Yeh, S. P. Liaw. Theoretical study of a fin subject to various types of heat transfer. Tatung Journal 20(1990), 59-66

[41] W. W. Lin, D. J. Lee. Boiling on a straight pin fin. AIChE J. 42(1996), 2721-2728

[42] W. W. Lin, D. J. Lee. Experimental study on pin fin boiling. Heat Transfer Science and Technology, Ed. B. X. Wang, Higher Education Pub. Beijing, 1996.

[43] H. C. Unal. An analytical study of boiling heat transfer from a fin. Int. J. Heat Mass Transfer 30(1987): 341-342

[44] W. W. Lin, D. J. Lee. Boiling on a straight pin fin with variable thermal conductivity. Heat and Mass Transfer 34 (1999) 381-386.

[45] M. G. Sobamowo, S. A. Ibrahim, M. O. Salami . A Study on Thermal Performance of Palladium as Material for Passive Heat Transfer Enhancement Devices in Thermal and Electronics Systems. Semiconductor Science and Information Devices. 2(2)(2020), 15-24.

[46] F. Khani, M. Ahmadzadeh Raji, H. Hamedi Nejad. Analytical solutions and efficiency of the nonlinear fin problem with temperature-dependent thermal conductivity and heat transfer coefficient. Commun Nonlinear Sci Numer Simulat 14 (2009) 3327–3338

[47] S. J. Liao. Beyond perturbation: introduction to the homotopy analysis method. Boca Raton (FL): Chapman & Hall/CRC Press; 2003.